

LINEAR STABILITY ANALYSIS AND APPLICATION OF A NEW SOLUTION METHOD OF THE ELASTODYNAMIC EQUATIONS SUITABLE FOR A UNIFIED FLUID-STRUCTURE-INTERACTION APPROACH

C. G. Giannopapa*

Dept. of Mathematics and Computer Science
Technische Universiteit Eindhoven
PO Box 513, 5600 MB Eindhoven
The Netherlands
Email: c.g.giannopapa@tue.nl

G. Papadakis

Experimental and Computational Laboratory for the
Analysis of Turbulence
Department of Mechanical Engineering,
King's College London, Strand WC2R 2LS, UK
Email: george.papadakis@kcl.ac.uk

*: Corresponding author

ABSTRACT

In the conventional approach for fluid-structure interaction problems, the fluid and solid components are treated separately and information is exchanged across their interface. According to the conventional terminology, the current numerical methods can be grouped in two major categories: partitioned methods and monolithic methods. Both methods use separate sets of equations for fluid and solid that have different unknown variables. A unified solution method has been presented in [1], which is different from these methods. The new approach treats both fluid and solid as a single continuum, thus the whole computational domain is treated as one entity discretised on a single grid. Its behavior is described by a single set of equations, which are solved fully implicitly. In this paper the elastodynamic equations are reformulated so that they contain the same unknowns as the Navier-Stokes equations, namely velocities and pressure. Two time marching and one spatial discretisation scheme, widely used for fluids equations, are applied for the solution of the reformulated equations for solids. Using linear stability analysis, the accuracy and dissipation characteristics of the resulting difference equations are examined. The aforementioned schemes are applied to a transient structural problem (beam bending) and the results compare favorably with available analytic solutions and are consistent with the conclusions of the stability analysis. A parametric investigation using different meshes, time steps and beam dimensions is also presented. For all cases examined the numerical solution was stable and robust and therefore is suitable for the next stage of application to full fluid-structure interaction problems.

Keywords: Fluid structure interaction, stability analysis, unified method, finite volume discretisation method

INTRODUCTION

Fluid structure interaction (FSI) occurs in many areas of engineering (aerospace, civil or mechanical) as well as other scientific disciplines including medicine, biomechanics etc.

The term FSI describes the influence of a fluid variable (for example pressure or temperature) on a solid and, crucially, vice versa. This interaction between the two components may be due to heat or momentum transfer or often a combination of the two. This paper is concerned with the interaction between a solid body and a fluid due to momentum transfer only. More specifically, is concerned with small local deformations of the solid rather than bulk deformations and rigid body motions as in [2].

During this interaction, the fluid normal and shear stresses act on the structure and cause it to deform. This deformation alters the flow domain and so it affects the fluid stress field. Thus, the response of the system can be determined only if the fully coupled problem is solved. This interaction can have an enormous effect on the speed of pressure wave propagation and becomes particularly important when the liquid is almost incompressible, in which case the deformation on the solid cannot be neglected [3]. The reliable prediction of pressure waves is important in liquid filled vessels such as arterial flow, impact on liquid filled containers, pipelines etc.

The different numerical techniques for the solution of the equations describing an FSI problem are classified according to the way the coupling is treated. Numerical methods can be grouped in three major categories: *partitioned methods*, *monolithic methods* and *single solution methods*. Figure 1 below assists the reader with the conceptual understanding of the single solution method and its differences from the conventional methods.

Partitioned methods

In partitioned methods, shown schematically in Figure 1a, the fluid and solid solution domains are partitioned, the equations for both components are solved alternatively and the enforcement of kinematic and dynamic conditions at the interface is asynchronous. Typically two separate software packages are used for modeling the solid and fluid components. Partitioning leads inherently to loss of conservation of properties of the continua (fluid and structure). The energy increase in the system leads to

instability, which is the major drawback of the method. An overview of the benefits and disadvantages of these methods can be found in [4].

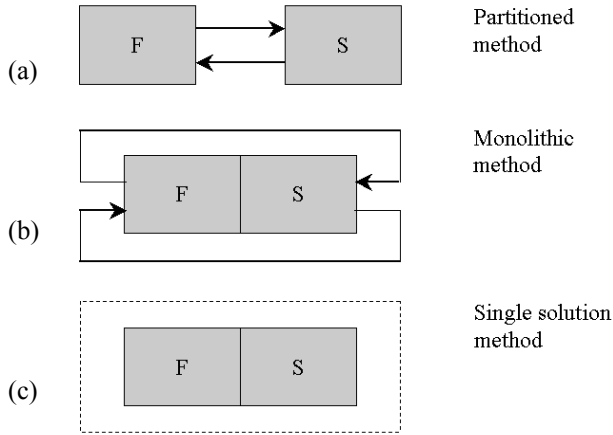


Figure 1: Classification of FSI methods

Monolithic methods

The monolithic methods, shown in Figure 1b, use two separate sets of equations for fluid and solid, couple the fluid dynamics and structural dynamics implicitly and solve the equations iteratively until convergence within each time step (synchronous interaction) [5]. These methods can be unconditionally stable and energy conserving when the modified Osher scheme is used for the fluid elements [6].

Single solution method

The single solution method [1,7] is a fully coupled method in which the fluid and solid are solved simultaneously for each time step in a single solution domain (Figure 1c). A single set of equations is used to describe the fluid and solid and their interface is contained within the solution domain itself making the coupling inherently implicit. The objective is to model fluid and solid simultaneously in a single solution environment and thus to eliminate stability problems associated with the segregated approach.

MATHEMATICAL FORMULATION

This paragraph is concerned with the presentation of the mathematical formulation of the unified method for the solution of the equations for solids and liquids as described in [1,7]. The resulting set of equations contains the three velocity components and pressure as unknown variables.

In the Eulerian reference frame the following equations describe continuous media and are thus valid for both solids and fluids.

Momentum equation (neglecting body forces):

$$\frac{\partial \rho U}{\partial t} + \nabla \cdot (\rho U U) = \nabla \cdot \sigma \quad (1)$$

Continuity equation (or mass conservation):

$$\frac{\partial \rho}{\partial t} + \nabla \cdot (\rho U) = 0 \quad (2)$$

The difference between solid and fluid lies in the constitutive equation for the stress tensor, σ . For linear elastic, or Hookean solid σ is given by:

$$\sigma = 2\mu\varepsilon + \lambda tr(\varepsilon)I \quad (3)$$

and for the linear viscous or Newtonian fluid is given by:

$$\sigma = 2\eta dev(\dot{\varepsilon}) - pI \quad (4)$$

where ε is the strain tensor ($\varepsilon = 1/2(\nabla D + \nabla D^T)$), $\dot{\varepsilon}$ is the strain rate tensor, $dev(\cdot)$ is the deviatoric part of a tensor and D is the displacement vector.

The density and pressure for both liquids and solids are linked with the barotropic relation:

$$\frac{\partial \rho}{\partial p} = \frac{\rho}{K} \quad (5)$$

where K is the bulk modulus. The definition of pressure for solids will be given later on. For small variations in pressure about a reference pressure p_0 , equation (5) can be linearised as:

$$\rho \approx \rho_0 [1 + (p - p_0)/K] \quad (6)$$

In order to get to a single set of equations, the stress tensor for the solids is written as a function of velocity and pressure. This is done in two steps: in the first step a velocity formulation is created from the standard displacement formulation and in the second step pressure is extracted by splitting the stress tensor to its deviatoric and hydrostatic parts.

In the development that follows, the displacements are assumed to be infinitesimally small. This makes various non linear terms (such as second order terms) in the strain tensor negligible. The book of Eringen [8] provides the expressions for the elements of the strain tensor that include non linear terms. The assumption of small deformations also simplifies the numerical simulations because the computational mesh remains fixed. On the other hand, for larger deformations an arbitrary Lagrangian-Eulerian approach is necessary in which the mesh moves, following the deformation of the solid. In order to account for the mesh motion, the convective term on the left hand side of equation (1) should include the mesh velocity.

Displacement formulation for solids

Using the definition of the strain tensor ($\varepsilon = 1/2(\nabla D + \nabla D^T)$) and substituting in equation (3), the stress tensor as a function of displacement is obtained:

$$\sigma = \mu \nabla D + \mu (\nabla D)^T + \lambda \text{tr}(\nabla D) I \quad (7)$$

The momentum equation can then be written as:

$$\frac{\partial \rho \left(\frac{\partial D}{\partial t} \right)}{\partial t} = \nabla \cdot [\mu \nabla D + \mu (\nabla D)^T + \lambda \text{tr}(\nabla D) I] \quad (8)$$

This is the standard equation for small displacements that is used in stress analysis for solids. In order to derive equation (8), it was assumed that the convection term in equation (1) is negligible for small deformations.

Velocity formulation for solids

Displacement can be obtained by integrating the equation $\frac{dD}{dt} = U$ using any integration method. In the present paper the Crank-Nicolson method is used (see Figure 2):

$$D = \int_{t_0}^{t+\Delta t} U dt = D_{\Sigma} + \frac{\Delta t}{2} [U^n + U^o] \quad (9)$$

where the superscripts (n) and (o) denote the new and old time step respectively.

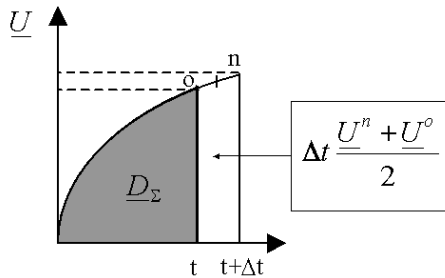


Figure 2: Integration of velocity

For the sake of readability the indices (o) and (n) are dropped from now on and so U denotes the velocity vector at the new time instant. Substituting (9) into equation (8), a velocity-based formulation is obtained:

$$\frac{\partial \rho U}{\partial t} = \frac{\Delta t}{2} \nabla \cdot [\mu \nabla U + \mu (\nabla U)^T + \lambda \text{tr}(\nabla U) I] + \nabla \cdot \Sigma^+ \quad (10)$$

where the tensor Σ^+ contains the contribution of the 'old' time instant. This is the end of the first step mentioned earlier. The next step is to extract pressure.

Velocity-pressure formulation for solids

The stress tensor σ can be split to its deviatoric and hydrostatic parts:

$$\sigma = \text{dev}(\sigma) - pI \quad (11)$$

i.e. pressure is defined as $p = -\frac{1}{3} \text{tr}(\sigma)$. This definition of pressure has been used in the past [9] in order to handle

incompressible solids and to avoid the node-locking problem. Substituting into the momentum equation we get:

$$\frac{\partial \rho U}{\partial t} = \frac{\Delta t}{2} \nabla \cdot \left[\mu \nabla U + \mu (\nabla U)^T + \frac{2}{3} \mu \text{tr}(\nabla U) I \right] + \nabla \cdot \text{dev} \Sigma^+ - \nabla p \quad (12)$$

This is the final form of the momentum equation for solids that contains velocity and pressure as unknowns.

It has to be mentioned at this point that the idea of describing the deformation of solids in terms of velocities is not new. Many papers in the literature [10-15] as well as the book of Leveque [16] describe how the hyperbolic system of elastodynamic equations can be written in terms of velocities and stresses. In the general three dimensional case there are nine unknowns (the three velocity components and the 6 independent components of the stress tensor). In the two dimensional case there are five unknowns (the two velocity components and the three stress components). Instead of the 6 stress components, some authors (for example Giese and Fey [13]) use the 6 independent strain components as unknowns; this leads to an equivalent system since there is a linear (and invertible) stress-strain relationship for Hookean solids. The resulting system is then solved using standard techniques suitable for hyperbolic systems such Godunov-type schemes and the method of characteristics. From the velocities, the displacements are then evaluated by integration. Displacements themselves do not appear in the above systems as they have been converted to velocities by taking the time derivative of the constitutive stress-strain relationship.

This is an elegant and consistent approach that is amenable to eigenanalysis for the evaluation of the propagation velocities of the elastic waves [16]. However, this formulation leads to a system with a large number of equations (9 as mentioned earlier for the general 3D case) but also most importantly such an approach can not be easily integrated with the Navier-Stokes equations that describe the motion of fluids. The reason is that the stresses in Newtonian fluids are uniquely determined by the velocities and only one additional variable, pressure. This means that if the aforementioned formulations for solids are used to solve a coupled fluid-structure interaction problem, some variables (velocities) will be evaluated in the whole domain, but from the rest of the variables, others will be evaluated in fluid domain (pressure) and others in the solid domain (6 stress components). There is no doubt that such approach can work but it can be quite cumbersome.

In the present paper, a different approach is followed. The elastodynamic equations for solids are reformulated in such a way as to contain velocities as well as pressure as independent variables. With this approach, all four variables will be evaluated in the whole domain. The pressure for solids is obtained from the trace of the stress tensor and in this way the pressure gradient term ($-\nabla p$) appears in the right hand side of the elastodynamic equation 12, in exactly the same form as in the Navier-Stokes equations. The remaining stresses are written in terms of displacements from

the constitutive stress-strain relationship. Note that the constitutive law is not differentiated in time (there is no need as we want to extract the pressure gradient term) and therefore the term Σ^* on the right hand side of the momentum equations contains displacements.

Although the present method was derived for infinitesimally small deformations, the methodology described to extract velocity and pressure can also be applied when the displacements are large. Of course in that case, care should be taken to use material constitutive laws that account for big deformations.

DISCRETISATION METHOD

The system of momentum and continuity equations needs to be solved numerically for the primitive variables of velocity and pressure. The finite volume (FV) method has been widely used in computational fluid dynamics for the solution Navier-Stokes equations but only in recent years in the area of stress analysis. However, since we seek a unified solution method, the finite volume method is used here for solids as well. The momentum equation in a semidiscretised form can be written as:

$$\alpha_p U_p = H(U) - \nabla p \quad (13)$$

where $H(U)$ contains the contributions of the surrounding nodes as well as all other source terms except pressure. Substituting equation (13) and equation (5) into the continuity equation (2) a new PDE for pressure can be obtained:

$$\frac{\rho}{K} \frac{\partial p}{\partial t} + \nabla \cdot \left[\frac{\rho}{\alpha_p} (H(U) - \nabla p) \right] = 0 \quad (14)$$

Velocity-pressure coupling

In order to ensure that the velocity field satisfies the continuity equation, the Pressure Implicit with Splitting of Operators (PISO) algorithm was adopted [17]. The PISO algorithm is most suitable for transient problems and can be used for compressible flows in an iterative manner. This solver has been widely used in fluids, but it can now be used for solids as well since we have the same pressure-velocity formulation.

Boundary conditions

The implementation of the boundary conditions for the fluids is well known. For the walls the no-slip condition is used as boundary condition for velocities while for pressure the normal pressure gradient is obtained by projecting the momentum equation to the wall normal vector [18, 19]. For solids there are two types of boundary conditions: prescribed displacement or traction. Care should be taken in the consistent implementation of these conditions for the reformulated solids equations, especially for the pressure equation. The first type (prescribed displacement) results in Dirichlet condition for velocity. For the second type (prescribed traction), the boundary condition for the momentum equation is obtained by applying force balance at

the boundary. For the pressure equation, the boundary condition is more complicated. Since this is the first time that such an equation is employed for solids, there is no information available in the open literature. In the present paper, the (vector) momentum equation is projected to the unit vector normal to the traction boundary and an expression for the pressure normal gradient is obtained that is used as boundary condition for the pressure equation. This approach is similar to the one used to extract the boundary condition for pressure for the incompressible Navier-Stokes equations as mentioned earlier but to the best of the authors' knowledge has never been applied for solids before.

STABILITY ANALYSIS

Having reformulated the equations for solids to resemble those of fluids and having selected a single discretisation method for both components, the next step is the selection of appropriate time marching and spatial discretisation schemes. In finite elements, one of the most widely used time advancement schemes for structural dynamic problems is the Newmark scheme which can provide very accurate and non-dissipative results if its coefficients are appropriately chosen. In the present paper, the time and spatial discretisation schemes selected for the reformulated equations for solids are identical to those widely used for the transient fluids equations. The purpose of this section is to assess the stability, accuracy and dissipation characteristics of these schemes when applied to the solids equations.

A number of methods exist to investigate the stability limits of a discretisation scheme. One such method is the Fourier or Von Neuman analysis [20]. This method is used to investigate the stability of the numerical method for the solution of the one-dimensional displacement equations used in the standard stress analysis and the one dimensional velocity equation developed and used in this paper.

Displacement formulation for solids

The standard stress analysis equation in one-dimension with the assumption of constant density is written as:

$$\frac{\partial^2 D_x}{\partial t^2} = c^2 \frac{\partial^2 D_x}{\partial x^2}, \quad t \in [0, \infty) \quad (15)$$

where c is the wave speed. This is the standard 1D wave equation. Using the first order Euler implicit difference to approximate the second order time derivative and the second order central approximation for the spatial derivatives, the following difference equation is obtained:

$$D_j^n - 2D_j^{n-1} + D_j^{n-2} = C_0^2 (D_{j-1}^n - 2D_j^n + D_{j+1}^n) \quad (16)$$

where the Courant number is $C_0 = c\Delta t/\Delta x$. The stencil of this Euler implicit scheme is shown in Figure 3a.

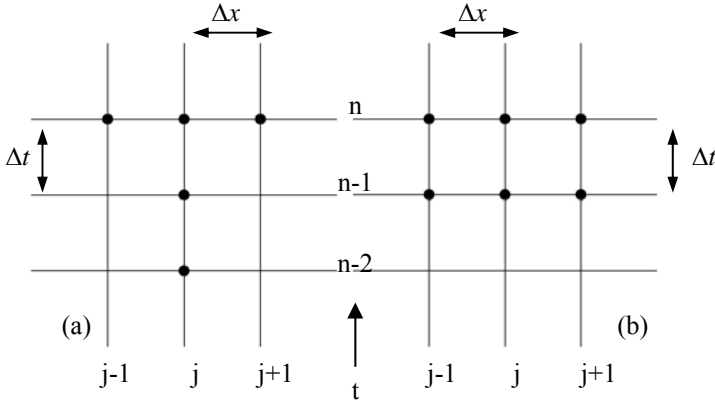


Figure 3: (a) Stencil for the 1D displacement formulation and (b) stencil of the 1D velocity formulation.

It is assumed that the solution of the finite difference scheme can be written as a Fourier series in complex, exponential form for any time level, n . After substitution, factorization and cancellation of the common terms the following characteristic (or dispersion) equation is obtained:

$$\left(1 + 4C_0^2 \sin^2 \frac{\alpha}{2}\right)G^2 - 2G + 1 = 0 \quad (17)$$

where G is the amplification factor between two consecutive time steps, $\alpha = 2\pi N$ and $N \in [2, \infty)$. Equation 17 has two solutions that correspond to opposite directions of propagation. The solution of equation 17 is:

$$G = \frac{1}{1 \pm i2C_0 \sin \frac{\alpha}{2}} \quad (18)$$

Velocity formulation for solids

The one-dimensional velocity formulation for solids, with the assumption of constant density, is equivalent to the following system of first order ordinary differential equations:

$$\frac{\partial U_x}{\partial t} = c^2 \frac{\partial^2 D_x}{\partial x^2} \quad (19)$$

$$\frac{\partial D_x}{\partial t} = U_x \quad (20)$$

For equation (19), the first order Euler implicit difference approximation is used to approximate the time derivative and for the spatial derivatives the second order central approximation is employed. These choices for the time marching and spatial discretisation schemes are very popular for the equations for fluids. The Crank-Nicolson method is used to integrate equation (20), as already mentioned. The system of Equations (19) and (20) after substitution of time and space approximations can be written as:

$$U_j^n - U_j^{n-1} = \frac{C_0^2}{\Delta t} (D_{j-1}^n - 2D_j^n + D_{j+1}^n) \quad (21)$$

$$D_j^n - D_j^{n-1} = \frac{\Delta t}{2} (U_j^n + U_j^{n-1}) \quad (22)$$

The stencil of this system of equations is shown in Figure 3b. Since now there are two coupled equations, the stability of the system is determined by the eigenvalues of the amplification matrix. The following characteristic (or dispersion) equation for the eigenvalues is obtained:

$$G^2 - \frac{2\left(1 - C_0^2 \sin^2 \frac{\alpha}{2}\right)}{1 + 2C_0^2 \sin^2 \frac{\alpha}{2}} G + \frac{1}{1 - 2C_0^2 \sin^2 \frac{\alpha}{2}} = 0 \quad (23)$$

where $\alpha = 2\pi N$ and $N \in [2, \infty)$. The analytical solution of equation (23) is:

$$G = \frac{1}{-2 - 2C_0^2 \sin^2 \frac{\alpha}{2} \pm \sqrt{2C_0^2 \sin^2 \frac{\alpha}{2} \left(2C_0^2 \sin^2 \frac{\alpha}{2} + 8\right)}} \quad (24)$$

The amplitude portraits for different Courant numbers $C_0 = 1/4, 1/2, 3/4, 1, 5/4$ and 2 in comparison with those of the displacement equation are shown in the following Figure 4. It can be seen that the time and spatial discretisation schemes used for the velocity formulation lead to an unconditionally stable method for all C_0 . The numerical damping (dissipation) is also smaller compared to the one added by the scheme used for the displacement equation.

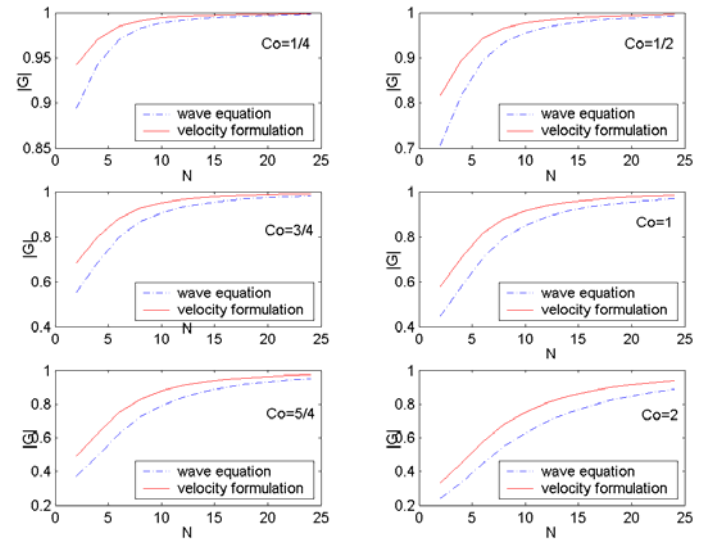


Figure 4: Comparison of amplitude portraits for the 1D velocity and displacement formulations.

In the following section the aforementioned schemes are applied for the solution of a two dimensional structural dynamic problem and the results are discussed in the light of the previous 1D linear stability analysis.

VALIDATION OF THE RESULTS

The mathematical model and the solution method are standard for compressible or incompressible fluid modeling, but as they are new for solids they need to be tested.

A transient beam-bending case is chosen to test the method. This case was chosen because apart from normal stress it comprises also shear stress. The effect of shear stress is of great importance in wave propagation, thus such a case would be a good validation tool. Figure 5 shows a schematic representation of the case considered.

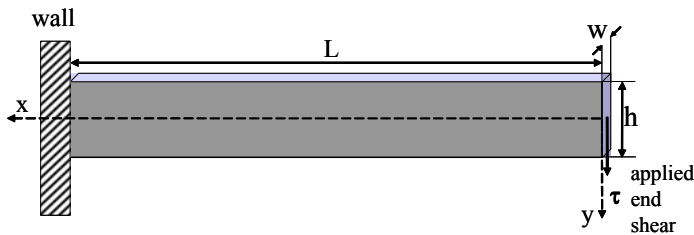


Figure 5: Two dimensional beam bending case.

The cantilevered beam is deflected from the horizontal position by applying at the right end a shear stress $\tau = 10^6 \text{ Pa}$ and is then released. The upper and lower surfaces of the beam are free traction boundaries. The beam specifications are shown in Table 1.

| Property | Value |
|---------------------------|----------------------------|
| Modulus (E) | $4 \times 10^9 \text{ Pa}$ |
| Poisson's ratio (ν) | 0.3 |
| Density (ρ) | 1450 Kg/m^3 |
| Length (L) | 20m |
| Height (h) | 5m |
| Depth (w) | 1m |

Table 1: Material properties and dimensions of the beam.

A two-dimensional analytical solution for the steady state of the maximum end displacement at $x=0$ is given by [21]:

$$\delta = \frac{4\tau L^3}{E h^2} \left[1 + \frac{3}{4}(1+\nu) \left(\frac{h}{L} \right)^2 \right] \quad (25)$$

In order to calculate the main frequency of oscillation of the beam, a one-dimensional approximation is used for which an analytical solution is available. Unfortunately a two dimensional solution for the frequency has not been found. Thus, the 1D solution is used only as a rough reference guide to validate the computational results. The fundamental eigenfrequency of the undamped oscillation is [22]:

$$\omega^2 = 1.875^4 \frac{Eh^2}{12\rho L^4} \quad (26)$$

For the present case, the end displacement is $\delta = 0.34\text{m}$, the oscillation frequency is $f = \omega/2\pi = 3.35 \text{ Hz}$ and the

propagation of the stress wave through the beam is $c = \sqrt{E/\rho} = 1660\text{m/sec}$.

RESULTS

The time integration scheme used for equation (12) was first-order Euler implicit. A 40×10 mesh was used with a time step 10^{-4}s corresponding to $Co=0.33$. Convergence was achieved using two PISO loops and four pressure-velocity loops for each time step. At $t=0$ the beam is horizontal and the displacement is equal to 0. All figures below show the displacement with respect to this initial position. For a static problem (i.e. when the beam does not oscillate), the displacement (δ) of the right end is given by equation 25. When the beam oscillates, it does so around the static location and the displacement varies between 0 and 2δ . The predicted frequency of oscillation is 3.32Hz while the maximum and mean (static) deflections of 0.62m and 0.31m, respectively. The computed values are quite close to the values from the analytical solution, which predicts a static deflection of 0.34m and an oscillation frequency of 3.35Hz, as already mentioned. A comparison between the standard displacement formulation and the new velocity-pressure formulation is shown in Figure 6. For the standard stress analysis formulation, the finite volume method was used with a second-order central discretisation scheme in space and a first-order accurate scheme in time. The results obtained using the two formulations agree quite well.

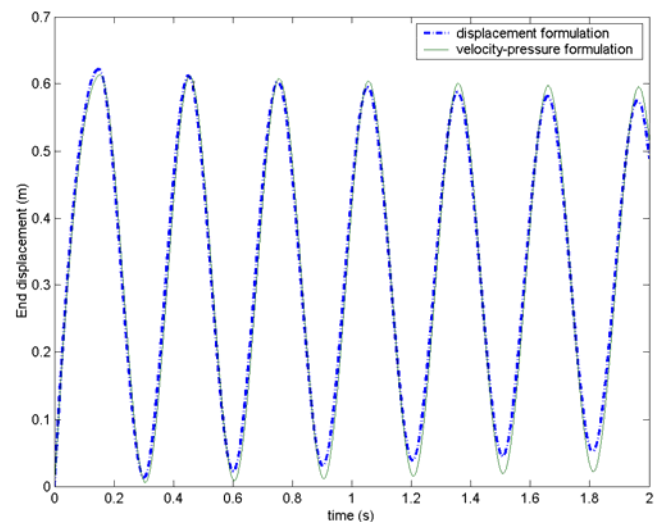


Figure 6: Comparison of end displacement obtained with the standard stress analysis and the velocity-pressure formulation ($Co=0.33$).

In order to investigate the numerical dissipation of the two methods, a calculation was performed until time $t=100\text{s}$. In a previous study [1], it was found that the standard stress analysis completely dissipates after 56 beam oscillations, whereas the velocity formulation has dissipated 33% after 332 oscillations. The reason for this behavior can now be explained from the conclusions of linear stability analysis presented earlier on. In Figure 4, it was shown that the present velocity formulation is less dissipative compared to the displacement formulation for all Courant numbers.

Clearly a more accurate time approximation would reduce the amount of dissipation in the standard formulation. For example, as already mentioned, the Newmark time integration scheme can provide very accurate and non-dissipative results [9,23].

The effect of the discretisation scheme used for the first order time derivative of velocity in equation 12 will now be investigated. The discretisation schemes compared are Euler Implicit and Backward Differencing (or three time level method). The latter is a second order accurate scheme and is also frequently used in computational fluid dynamics. In Figure 7 it can be seen that the Backward Differencing scheme is less dissipative than the Euler implicit, as expected. Over a period of 30s (300,000 time steps, 100 oscillations) the Euler Implicit dissipated about 14.7% and over 100s (1,000,000 time steps, 332 oscillations) about 33.3%. On the other hand the Backward Differencing over a 30 s period has much smaller dissipation.

The accuracy can be improved further with the decrease of the time step size. Figure 8 compares different time step sizes for Euler Implicit discretisation scheme. It can be seen that when the time step is decreased from 10^{-4} s to 10^{-5} s ($C_0=0.033$) the accuracy over a 30s period improves about 7.5 %. When the time step is decreased from 10^{-5} s to 10^{-6} s ($C_0=0.0033$) there is no significant change, only 0.62% improvement, but the computational overhead is quite substantial.

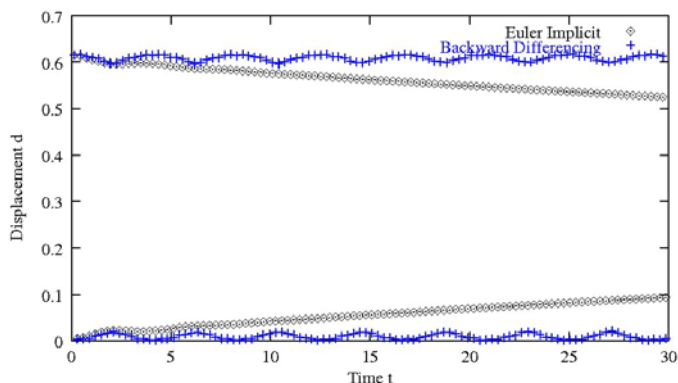


Figure 7: Comparison of Euler Implicit and Backward Differencing scheme (envelope of end displacement).

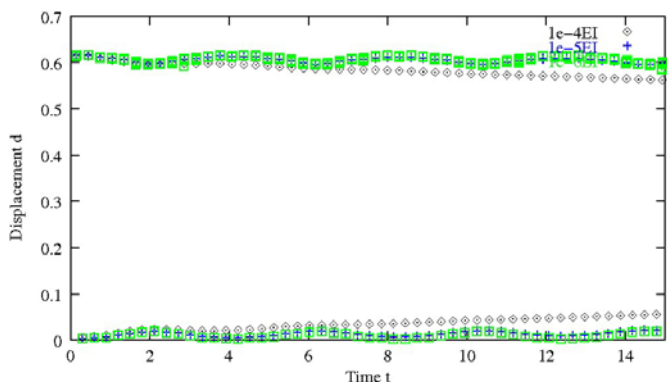


Figure 8: Effect of time step on the envelope of end displacement (Euler Implicit scheme with time steps 10^{-4} s, 10^{-5} s and 10^{-6} s).

The results of the first order accurate Euler Implicit scheme with a decreased time step can be compared with those of the second order accurate Backward Differencing scheme. Figure 9 illustrates that for a period of 30s the results of Backward Differencing with time step 10^{-4} s and Euler Implicit with time step 10^{-5} s are almost identical. The Backward differencing scheme with 10^{-4} s time step is 1.2% less dissipative than the Euler Implicit with 10^{-5} s time step. In conclusion, from the two time differencing schemes, backward differencing is more accurate and converges faster to a time-step independent solution. On the other hand the values of velocities at two previous time steps need to be stored which increases somewhat the memory requirements.

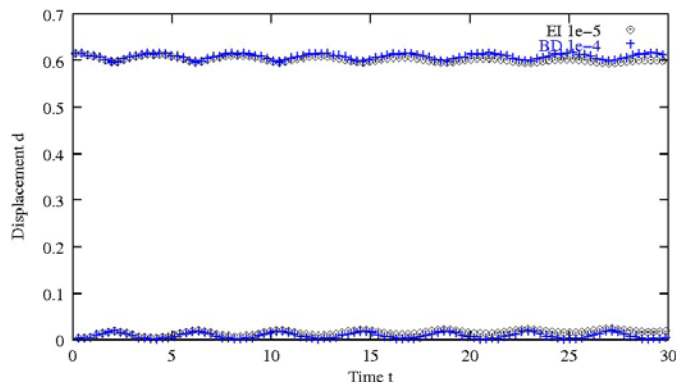


Figure 9: Comparison of envelope of end displacement obtained with Euler Implicit (time step 10^{-5} s) and Backward differencing (time step 10^{-4} s).

In figure 9, the envelope of the Backward Differencing scheme exhibits repeatable beats. The beats can be either physical or numerical and related to the discretisation of the computational domain. If these beats are physical they can only represent the first eigenmode of the vibration. In order to investigate this, the two-dimensional beam bending case was run using ANSYS finite element commercial package. The beats appearing in the envelope of the displacement of our discretisation have a frequency of 0.2369 Hz, where the frequency of the first mode found by ANSYS is 0.677 Hz. Thus, it can be concluded that their appearance is of numerical nature. In Figure 9, the beats are independent of time step size.

The effect of mesh size on the beats is also investigated. The mesh resolution presented up to now has been 40×10 cells. Two finer mesh resolutions, 60×20 and 200×50 , were also examined. The time step size is kept the same ($\Delta t = 10^{-4}$ s) and the discretisation scheme for the temporal term is Backward differencing. The results are presented in Figure 10.

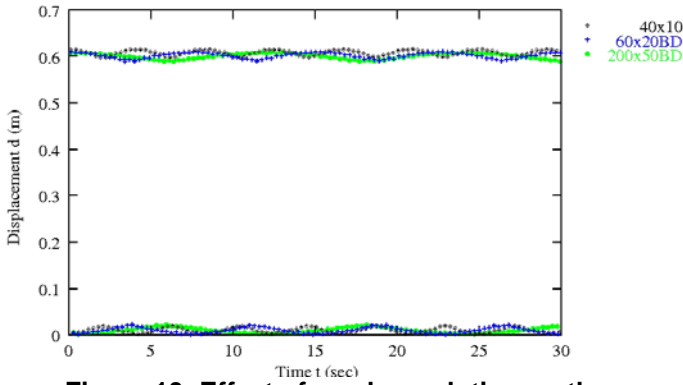


Figure 10: Effect of mesh resolution on the envelope of end displacement (meshes 40x10, 60x20 and 200x50).

Beats appear in the displacement envelope in all cases examined but their number decreases with the increase of the mesh resolution. The frequency of the beats in the 40x10 cells mesh is 0.1148 Hz, while for the 60x20 reduces to 0.1309 Hz and for 200x50 drops down to 0.0782Hz, thus almost disappear (only two beats in 300,000 time steps corresponding to 100 oscillations).

| Variable | Analytical | Predicted | % Difference |
|--|------------|-----------|--------------|
| <i>Beam dimensions: 10mx5m; end shear: 10⁶ Pa</i> | | | |
| Max Displacement [m] | 0.0995 | 0.0866 | 12.96 |
| Frequency [Hz] | 13.41 | 11.64 | 13.29 |
| <i>Beam size: 20mx5m; end shear: 10⁶ Pa</i> | | | |
| Max Displacement [m] | 0.68 | 0.62 | 8.82 |
| Frequency [Hz] | 3.35 | 3.32 | 0.9 |
| <i>Beam size: 40mx5m; end shear: 10⁶ Pa</i> | | | |
| Max Displacement [m] | 5.2 | 4.72 | 9.21 |
| Frequency [Hz] | 0.84 | 0.86 | 2.05 |
| <i>Beam size: 20mx5m; end shear: 5·10⁵ Pa</i> | | | |
| Max Displacement [m] | 0.34 | 0.313 | 7.94 |
| Frequency [Hz] | 3.35 | 3.29 | 1.79 |

Table 2: Comparison between analytical and computational solutions for beams with different dimensions and loading conditions.

A parametric study was also undertaken with different beam dimensions and end load. The conditions, the predicted and analytic results as well as their differences are shown in table 2. In all cases the time step used was $\Delta t=10^{-4}$ s, the temporal discretisation scheme applied was Backward differencing and the mesh resolution Δx was kept constant. For example, for the case with 10m beam length the mesh used was 20x10cells. The end displacement is shown in figure 11. The percentage differences between the analytic solution and the predictions for this case are slightly above 10% as shown in Table 2. It must be noted however that as the analytical solution is 1D, the shorter the beam is in relation to its height, the less accurate the solution would be.

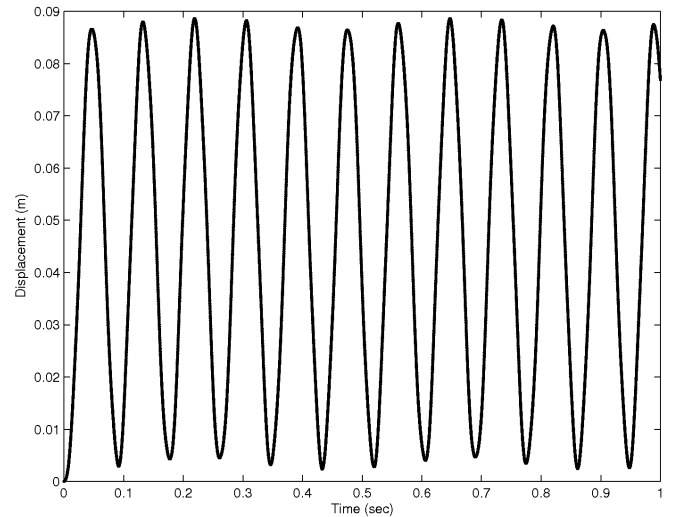


Figure 11: End displacement for a beam with dimensions 10mx5m.

For the case with double the beam length (40mx5m) the mesh used was 80x10cells (Figure 12). The maximum end displacement was 4.72m and the frequency was 0.86 Hz. The percentage difference between the analytical and the numerical solution is 2.05 % for the frequency and 9.21% for the displacement (Table 2).

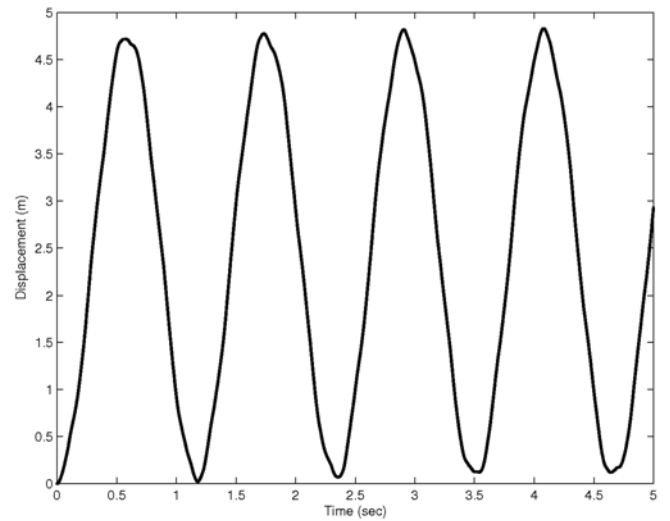


Figure 12: End displacement for a beam with dimensions 40mx5m.

In the case where the applied end shear was halved ($\tau=5 \cdot 10^5$ Pa) the mesh resolution was 40x10 cells, the same as the one in the base case. Figure 13 presents the results. The maximum end displacement is 0.313m and the frequency of the oscillation of the beam is 3.29 Hz i.e. the frequency does not depend on the applied load. The percentage difference for the frequency between the analytical solution and the numerical solution is 1.79 % and for the maximum displacement is 7.94 % (Table 2).

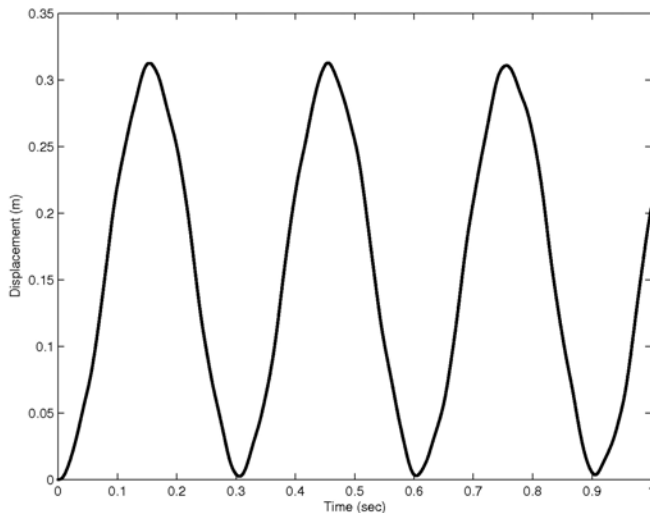


Figure 13: End displacement for a beam with dimensions 20mx5m and applied end shear $\tau=5 \cdot 10^5$ Pa.

IMPLEMENTATION IN FSI

The method can be directly used in a fluid-structure interaction problem to create an algorithm where a single mesh and a unified method is used for both fluids and solids. The grid cells will hold an extra property defining the phase of the medium, i.e. whether it is a fluid or a solid. In that way according to the phase, the appropriate material properties associated with the state of the continuum will be used. This is the subject of future work.

CONCLUSIONS

The single solution method suitable for fluid-structure interaction problems is general, with no approximations made to the basic continuum model for Hookean solids and Newtonian fluids.

The principal idea is that the fluid and structural analysis is performed by a single set of equations in a single solution domain, in a fully implicit and coupled manner. The single set of equations has as primitive variables velocity and pressure. The pressure-velocity coupling is handled using the PISO algorithm. Note also that since pressure is used as an independent variable, the study of structural deformations of fully incompressible solids is straightforward while well-known problems such as node locking [24] are avoided.

The unified solution method for FSI was applied in this paper against a transient beam bending case. The discretisation method was stable and less dissipative than the standard stress analysis discretisation method used. This was in agreement with the one-dimensional linear stability analysis.

The comparison of the Backward differencing with Euler implicit for the discretisation of the temporal term showed that the former introduces smaller amounts of dissipation and gives more accurate results. The decrease of the time step size by a factor of 10 for the Euler implicit improves the accuracy and brings the results closer to those of Backward differencing.

The results showed that the unified solution method is capable of solving standard solid mechanics problems with

sufficient accuracy. The next step of this work is the application of this method to full FSI problems and comparisons with existing partitioned and monolithic methods.

ACKNOWLEDGMENTS

The authors would like to thank EPSRC (research grant GR/N65769) for funding this project and Nabla Ltd.

NOMENCLATURE

Roman symbols

| | | |
|------|-----|----------------|
| Co | - | Courant number |
| D | m | displacement |
| f | Hz | frequency |
| F | - | fluid |
| h | m | height |
| I | - | unit tensor |
| K | Pa | bulk modulus |
| L | m | length |
| p | Pa | pressure |
| S | - | solid |
| t | s | time |
| U | m/s | velocity |

Greek symbols

| | | |
|---------------|----------|------------------------------------|
| Δt | s | time step |
| Δx | m | grid spacing |
| ε | - | strain tensor |
| E | Pa | Young's modulus |
| η | m^2/s | dynamic viscosity |
| λ | Pa | Lame's coefficient |
| μ | Pa | Lame's coefficient |
| ν | - | Poisson ratio |
| ρ | kg/m^3 | density |
| σ | Pa | Cauchy stress tensor |
| τ | Pa | applied end shear |
| ω | Hz | frequency of undamped oscillations |

REFERENCES

- [1] Giannopapa, C. G. and Papadakis, G. (2004) "A new formulation for solids suitable for a unified solution method for fluid-structure interaction problems", ASME PVP 2004, San Diego California, July, PVP-Vol. **491-1**, pp. 111-117.
- [2] Wiggert, D. C., and Tijsseling, A. S. (2001) "Fluid transients and fluid-structure interaction in flexible liquid-filled piping", ASME Applied Mechanics Reviews, **54**, pp. 455-481.
- [3] Korteweg, D. J. (1878) "Über die Fortpflanzungsgeschwindigkeit des Schalles in elastischen rohen", Annalen der Physik und Chemie, **5**, pp. 525-542.
- [4] Felippa, C. A., Park, K. C. and Farhat, F. (2001) "Partitioned analysis of coupled mechanical systems", Computer methods in applied mechanics and engineering, **190**, pp. 3247-3270.

- [5] Hübner, B., Walhorn, E., and Dinkler, D. (2004) “A monolithic approach to fluid-structure interaction using space-time finite elements”, *Computer methods in applied mechanics and engineering*, **193**, pp. 2087-2104.
- [6] van Brummelen, E. H. and Koren, B. (2003) “A pressure-invariant conservation godonov-type method for barotropic two-fluid flows”, *Journal of computational physics*, **185**, pp. 289-308.
- [7] Giannopapa, C. G. (2004) *Fluid-Structure interaction in flexible vessels*, PhD thesis, University of London.
- [8] Eringen, A. C. (1989) *Mechanics of continua*, Robert E. Krieger Publishing Company.
- [9] Bathe, K. J. (1997) *Finite element procedures*, Prentice Hall, Englewood Cliffs, New Jersey.
- [10] Vardy, A.E. and Alsarraj, A.T. (1989) “Method of characteristics analysis of one-dimensional members”, *Journal of Sound and Vibration*, **129**(3), pp. 477-487.
- [11] Vardy, A.E. and Alsarraj, A.T. (1991) “Coupled axial and flexural vibration of 1-D members”, *Journal of Sound and Vibration*, **148**(1), pp 25-39.
- [12] Lin, X. and Ballman, J. (1995) “A numerical scheme for axisymmetric elastic waves in solids”, *Wave Motion*, **21**, pp. 115-126.
- [13] Giese, G. and Fey, M. (2002) “A genuinely multidimensional high-resolution scheme for the elastic-plastic wave equation”, *Journal of Computational Physics*, **181**, pp. 338-353.
- [14] Voinovich, P., Merlen, A., Timofeev, E. and Takayama, K. (2003) “A Godunov-type finite volume scheme for unified solid-liquid elastodynamics on arbitrary two-dimensional grids”, *Shock Waves*, **13**, pp. 221-230.
- [15] Voinovich, P. and Merlen, A. (2003) “Two-dimensional unstructured elastic model for acoustic pulse scattering at solid-liquid interfaces”, *Shock Waves*, **13**, pp. 421-429.
- [16] Leveque, R. J. (2002) *Finite volume methods for hyperbolic problems*, Cambridge University Press.
- [17] Issa, R. I. (1986) “Solution of the implicit discretised fluid flow equation by operator-splitting”, *Journal of Computational Physics*, **62**, pp. 40-65.
- [18] Gresho, P.H. and Sani, R.L. (1987) “On pressure boundary conditions for the incompressible Navier-Stokes equations”, *International Journal for Numerical Methods in Fluids*, **7**, pp. 1111-1145.
- [19] Ferziger, J. H. and Peric, M. (1996) *Computational methods of fluid dynamics*, Springer-Verlag, Berlin, Germany.
- [20] Mattheij, R. M. M., Rienstra, S. W., and tenTije Boonkamp, J. H. M. (2005) *Partial differential equations: modeling, analysis and computing*, SIAM, Philadelphia (in Press).
- [21] Case, J., Chilver, A. H. and Ross, C. T. F. (1999) *Strength of Materials and Structures*, Arnold, New York.
- [22] Geradin, M., and Rixen, D. (1997) *Mechanical vibrations*, Wiley, Chichester, UK.
- [23] Sloan, A. K., Bailey, C., and Cross, M. (2003) “Dynamic solid mechanics using the finite volume methods,” *Applied mathematical modeling*, **27**, pp. 69-87.
- [24] Bath, M., and Kamm, R. D. (1999) “A fluid structure interaction finite element analysis of pulsatile blood flow in arterial structures”, *Transactions of ASME- Journal of Biomechanical Engineering*, **121**, pp. 361-369.